High throughput and machine learning approaches for thermoelectric materials

Eric S. Toberer,* Andrew Novick, and Elif Ertekin

Over the past decade, the search for new thermoelectric materials has shifted profoundly, from reliance on experimental serendipity to computationally guided discovery. This transformation is particularly challenging due to the complexity of the terms governing thermoelectric performance, including dopability, electronic structure, scattering mechanisms, and thermal conductivity. In this article, we frame thermoelectric discovery as a two-stage design challenge: identifying compounds with high thermoelectric potential and then optimizing their performance through dopants, defects, and alloying. The first stage benefits from automated screening pipelines based on density functional theory, while the second relies on finer-grained models that capture local structural motifs, complex scattering mechanisms, and alloy thermodynamics. Advances in machine learning and artificial intelligence have revolutionized every stage of this design process, providing inexpensive surrogates, uncertainty quantification, and access to mechanistic insights.

Introduction

The discovery of a truly high-efficiency thermoelectric material would be transformative, enabling all-solid-state semiconductor solutions for both refrigeration and power generation–potentially replacing small-scale mechanical heat engines and vapor-compression cooling systems. The breakthroughs of such an advance would rival those of high-temperature superconductivity and rechargeable batteries in their technological significance. And yet, despite intensive research since the mid-20th century, achieving high thermoelectric performance remains an intricate puzzle. While the figure of merit, zT, encapsulates the desired electronic and thermal-transport properties in a single metric, tuning one transport parameter often affects the others in conflicting ways. This delicate balance between electrical conductivity, the Seebeck coefficient, and thermal conductivity rests atop a multitude of material design decisions.

The foundational questions we seek to answer in thermoelectric materials discovery and design revolve around dynamical processes in the solid state, namely, the diffusion of charge and heat. We wish to control the energy dependence of the diffusion coefficient, $\mathcal{D}(E)$, and the density of states, $g(E)$, of both electronic carriers and phonons. Further, for electronic carriers, the Fermi level must be precisely placed for optimal performance. In crystalline materials, diffusion coefficients are typically expressed in terms of the group velocity, v, and relaxation time, τ, of the relevant carrier (phonon or electron). To highlight the similarity in electron (σ) and phonon (κ_L) conductivity, Equations 1 and 2 are provided for isotropic solids:

$$\sigma = \frac{-q^2}{3}\int \frac{df_{FD}}{dE} g v^2 \tau dE, \tag{1}$$

$$\kappa_L = \frac{1}{3}\int E \frac{\partial f_{BE}}{\partial T} g v^2 \tau dE. \tag{2}$$

Here, f_{FD} and f_{BE} refer to the Fermi Dirac and Bose Einstein distribution functions. Note that g, v, and τ have the same formal definitions in the two equations, but refer to either electrons or phonons, depending on the context. Further, the Seebeck coefficient, S, is simply a modification of the electronic conductivity:

$$S = \frac{q}{3\sigma T}\int (E - E_F)\frac{df_{FD}}{dE} g v^2 \tau dE. \tag{3}$$

Eric S. Toberer, Department of Physics, Colorado School of Mines, Golden, USA; etoberer@mines.edu
Andrew Novick, Department of Physics, Colorado School of Mines, Golden, USA; novick@mines.edu
Elif Ertekin, Mechanical Science and Engineering, The Grainger College of Engineering, University of Illinois at Urbana-Champaign, Urbana, USA; ertekin@illinois.edu
*Corresponding author
doi:10.1557/s43577-025-00956-1

© The Author(s), under exclusive License to the Materials Research Society 2025

Figure 1 shows the impact of the constituent terms on thermoelectric transport. Conceptualizing transport in terms of the energy dependence of g, v, and τ proves to be a valuable approach to material design.

Experimentally resolving a material's thermoelectric potential is laborious for a single composition, let alone across multiple compositions and crystal structures. Furthermore, as Figure 1 highlights, the experimental observables are scalar quantities that do not provide ready access to the integrands in Equations 1–3. First-principles computational approaches such as density functional theory (DFT) naturally offer insight into the reciprocal space processes that govern these terms; further, defect calculations can identify the range of Fermi level positions available.[1] The resulting comprehensive evaluation yields key predictions of zT and its dependence on carrier concentration, presenting clear optimization strategies for experimentalists. **Figure 2** shows that modern computational methods can predict zT with sufficient accuracy to guide experimental efforts.

The task of high-throughput computational studies is to find ways, both with artificial intelligence/machine learning (AI/ML) and physics-informed analytical modeling, to accelerate predictions such that similar levels of predictive fidelity can be accomplished across diverse sets of potential structures. Over the last two decades, the field has devoted immense effort to computationally guided exploration. In this article, we find it useful to separate computational guidance into two stages.

- First, models that estimate the ultimate thermoelectric potential of a material. Beginning with either known or hypothetical materials, this modality can screen large swaths of candidates for further investigation (experimental or computational).

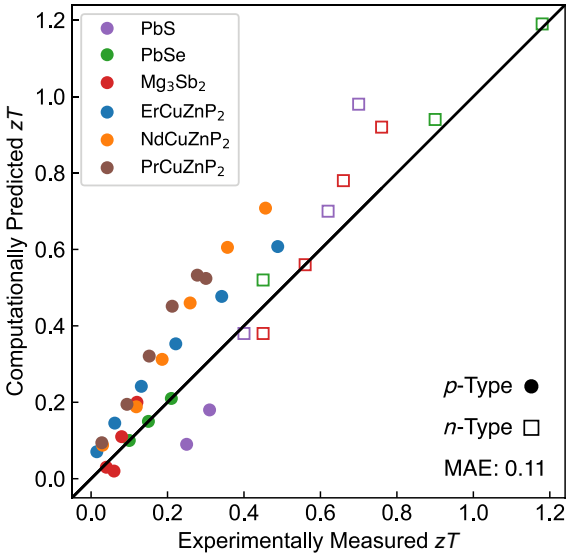

Figure 2. With the incorporation of energy-dependent scattering calculations, predicted thermoelectric performance is now within the intrinsic uncertainty of experimental zT measurements. Note that these calculations invoked the ability to dope to a particular carrier concentration rather than having that be part of the workflow. Reprinted with permission from References 2 through 8.

- Second, the implementation of computational models to explore the vast design spaces involved in doping and alloying. In this stage, computation recommends specific synthesis conditions for optimal performance.

This design paradigm can be viewed as an hourglass (**Figure 3**a), where the search space is initially broad, narrows down to a target material, and then expands again. While the

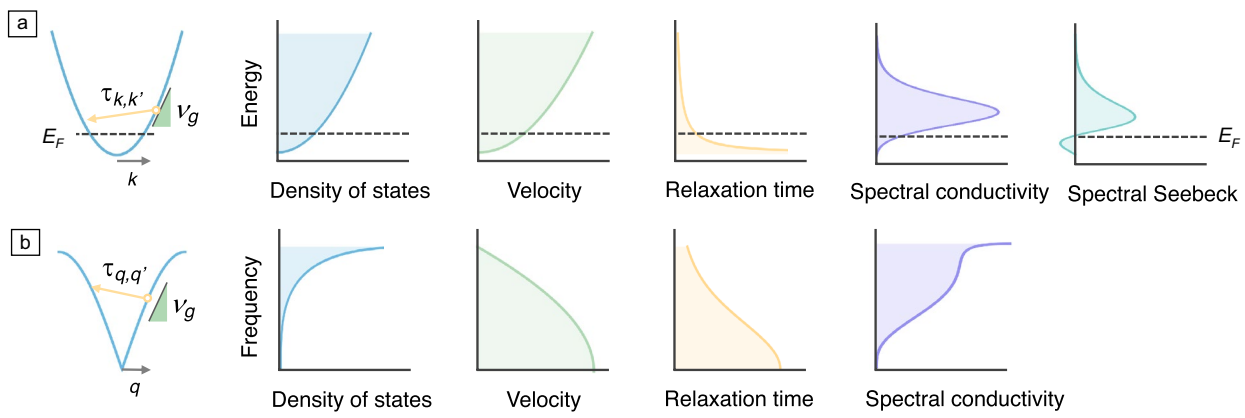

Figure 1. (a) The electronic properties of a semiconductor readily emerge from a reciprocal space view of transport within the relaxation time approximation. The spectral conductivity and spectral Seebeck refers to the integrands of Equations 1 and 3. As the $(E - E_F)$ term can lead to both positive and negative values, the energy dependence of the spectral conductivity is vital in determining the magnitude of the Seebeck coefficient. (b) Thermal transport shows similar dependencies within the integrand of Equation 2. Here, multiple scattering sources are considered within the phonon relaxation time. Accurately and efficiently predicting all of these properties across a broad range of structures or alloy compositions is a persistent challenge.

first stage has been a major focus of thermoelectric material design since the 2010s, the second stage has been steadily gaining momentum. This progression is a natural product of the numerous design variables available and the precision required in their tuning. Every stage of design has opportunities for the incorporation of AI/ML-based predictive surrogates (Figure 3b) or to more efficiently guide the search process.

The early days of computation

Across materials science, computational efforts typically begin by building trust through explaining experimental observations. In thermoelectric materials, this took the form of predicting Seebeck coefficient, electronic mobility, and lattice thermal conductivity.[9,10] By the mid-2000s, Boltzmann transport-based codes such as BoltzTraP were developed to model electronic transport from DFT calculations with only modest fitting to experimental measurements. By systematically considering states across the Brillouin zone, these efforts typically performed an admirable job in determining charge carrier group velocity and density of states as well as anisotropic effects. However, scattering was typically treated with a constant relaxation time approximation for all electrons or phonons.

This simplification is understandable, as there are a multitude of pairwise combinations of scattering sources and final states for a given electron. Further, these early efforts focused on perfectly periodic, well-known thermoelectric materials, and avoided questions of dopability (i.e., Fermi level control) and synthesizability. Nevertheless, these studies laid the groundwork for high-throughput efforts by establishing both the computational framework and trust in DFT-based transport predictions.

First search

The earliest high-throughput search for thermoelectric materials provides a superb pedagogical example of the opportunities and challenges therein. In 2006, Madsen screened 570 compounds across a diverse structural space of binary and ternary compounds containing Zn and Sb.[11] The electronic component of thermoelectric performance was predicted as a function of the Fermi level, assuming a universal charge carrier relaxation time across all materials. Such approximations were necessary due to the challenges at the time in estimating dopability ranges and scattering rates from phonons and defects. All materials were assumed to possess a rather conservative lattice thermal conductivity of 2 W/mK. This approach returned *n*-type LiZnSb as the most promising candidate, owing to an electronic structure that provided many high velocity transport channels. Specifically, LiZnSb's symmetry creates a conduction-band edge with six degenerate valleys, each highly anisotropic. With two decades of hindsight, the nuance incorporated into this early effort remains remarkable.

Computational guidance does not end at identifying a singular material; as Figure 3 highlights, the second stage concerning the interplay between native defects, dopants, and alloying is vital. In the case of LiZnSb, experimental efforts to realize its potential as an *n*-type material were stymied by its persistent *p*-type character.[12] Indeed, subsequent defect calculations showed that lithium vacancies act as "killer defects" that pin the Fermi level to the valence-band edge.[13] It is perhaps regrettable this critical lesson has seldom been fully integrated into more recent high-throughput search efforts.

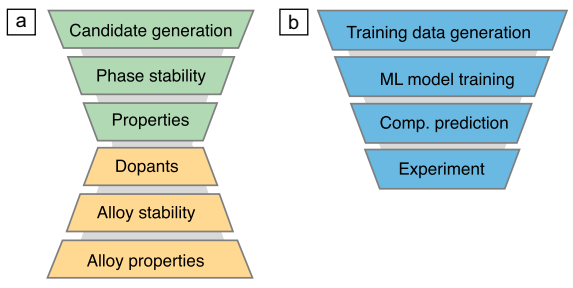

Figure 3. (a) Having generated a large suite of candidate compounds, the thermoelectric search space initially narrows down to promising materials. The consideration of both dopants and alloys re-expands the search. (b) At each stage, a machine learning (ML)-based model may be developed, refined, and experimentally validated.

Thermoelectric material screening

By the 2010s, major advancements were occurring in high-throughput computational infrastructure, enabling the automated prediction of stability, electronic structure, and transport properties in crystalline materials.[14–17] Much of this progress was driven by parallel searches for new energy materials such as photovoltaics, batteries, and catalysts. In the following, we break down the process of high-throughput thermoelectric search into five key steps: (1) defining a search space, (2) assembling a training data set, (3) featurizing the data set, (4) developing models to predict performance, and (5) applying analysis techniques to reveal insight into thermoelectric material design. When executed successfully, this first stage of search will reveal new opportunities for deeper exploration within a single material or small subset of materials.

Defining material search spaces

Early searches for thermoelectric materials spanned tens of thousands of known crystalline compounds, the vast majority of which had never been considered for thermoelectric performance.[18–21] By leveraging known crystal structure databases (e.g., the Inorganic Crystal Structure Database), these studies circumvented questions of phase stability. As screening methods continue to improve and new materials are experimentally discovered, this set of known structures continues to be a valuable space to revisit.

However, these materials represent only the tip of the iceberg–not only do vast numbers of ternary and quaternary compounds remain to be discovered,[22] but semimetals and metals

also enable alternative transport design strategies.[23,24] Furthermore, alloying has produced many of the top-performing thermoelectrics, motivating continued searches to navigate the continuous composition spaces inherent to alloys.

Multiple approaches are possible for seeking new candidate materials beyond what is found in crystal structure databases. One common method is to begin with a set of known crystal structures and apply chemical substitutions to realize compositions that have not previously been explored. This approach has been demonstrated in several material families, such as ABX, $CaAl_2Si_2$, ABX_4, and half-Heuslers.[25,26] Here, further complexity can be unlocked with symmetry-aware partial substitutions.[22] More recently emerging approaches include random structure search in which stable atomic structures can be discovered by randomly sampling and optimizing candidate configurations,[27–30] and crystal generative models that learn to create new structures similar to those they were trained on.[31–34]

Before embarking on an experimental campaign, candidate materials in the selected search space should be screened for phase stability using metrics such as proximity to the convex hull. The emergence of large material thermodynamics databases[35–39] are crucial for providing insight into competing phases and stability. Even so, it is difficult to say with certainty that a proposed compound lies on the convex hull. Uncertainties arise because of the imperfect accuracy of DFT, neglect of entropic effects at finite temperature, and the reality that the known hull is incomplete.

Training data

Robust predictive models for thermoelectric transport are built upon training data. One approach is to train models on experimental measurements of transport properties or derived quantities therein. Such data sets can range from small and heavily curated[19,40] to larger and more heterogeneous.[41] Heterogeneity arises from variation in sample form (e.g., thin film, polycrystalline, single crystal), processing techniques (e.g., spark plasma sintering), and doping level. The proper choice of predictive model will depend heavily on the heterogeneity and size of the data set.

With increasing computational power and more efficient codes, we are now seeing the rise of sizable computational data sets created specifically around thermoelectric transport.[2,42,43] While these training data sets originally focused on ground state DFT properties, they are increasingly considering scattering. This is remarkable, as electron–phonon scattering calculations using perturbation theory have traditionally been quite costly for even a single compound.[44] Most notable is the emergence of Ab initio Scattering andTransport (AMSET) to estimate charge carrier scattering (**Figure 4**).[45] *Ab initio* Scattering andTransport (AMSET) employs models for various scattering mechanisms, such as acoustic deformation potential and polar optical phonon scattering, using inputs like phonon frequencies and dielectric constants. This methodology significantly reduces computational cost while maintaining accuracy, enabling high-throughput screening of materials on standard computing resources. For example, Al-Fahdi et al. used the Ab initio Scattering andTransport (AMSET) code to calculate scattering rates and power factors for a set of 1937 materials,[2] while Fan et al. built a data set for the power factor of 796 chalcogenides using similar methods.[43] In both cases, these calculations formed training sets for machine learning models that classified whether a candidate material would have a sufficiently high power factor.

Featurization

Given some vast search space, inexpensive input features are necessary to drive a predictive model. Thermoelectric transport is largely driven by features in the electronic and phononic reciprocal spaces, and DFT is foundational for accessing such features.[21] For electronic transport, early efforts focused on band effective mass, band degeneracy, Fermi surface complexity, scattering channels, nested bands, and bulk modulus.[19,20,47,48] More recent efforts continue to find that features such as bandgap, band effective mass, and band degeneracy are critical descriptors for predicting electronic transport.[43]

Likewise, features from the phonon dispersion (e.g., maximum phonon frequency at the gamma point, speed of sound, higher order force constants) enable inexpensive surrogates for lattice thermal conductivity.[40,49] As lattice thermal conductivity is intrinsically tied to electronic structure through the energy required to distort chemical bonds, electronic descriptors are also used to predict thermal conductivity. For example, antibonding states a near the valence-band edge and lone pairs can be hallmarks of compounds with high bond anharmonicity.[50,51] For flexible thermoelectric applications, components of the elastic tensor are incorporated to assess the flexibility of van der Waals chalcogenides, with materials such as $NbSe_2$ Br_2 emerging from these targeted searches.[52] Given their ostensibly free cost, features derived from the elemental properties are commonly used.[2,42,52,53]

Featurizing crystal structures for thermoelectric materials design remains a persistent challenge. Simple structural descriptors such as the number of atoms in the unit cell, volume per atom, or summary statistics of the radial distribution function have been used[42,43] due to their simplicity, but may not capture the full complexity of solid-state bonding environments. More expressive representations treat the crystal structure as a graph, enabling the use of crystal graph convolutional neural networks (CGCNNs).[54] Recent advances introduce equivariant neural networks that respect the symmetries of three-dimensional space, leading to improved training efficiency and accuracy.[55,56] While these graph-based models are often applied to predict thermodynamic quantities,[22,57] they have also shown promise in modeling thermal conductivity and phonon scattering processes relevant to thermoelectric performance.[42,43]

An emerging alternative approach to materials representation leverages natural language processing (NLP) techniques by encoding crystal structures and compositions as descriptive text, then embedding them into a high-dimensional latent

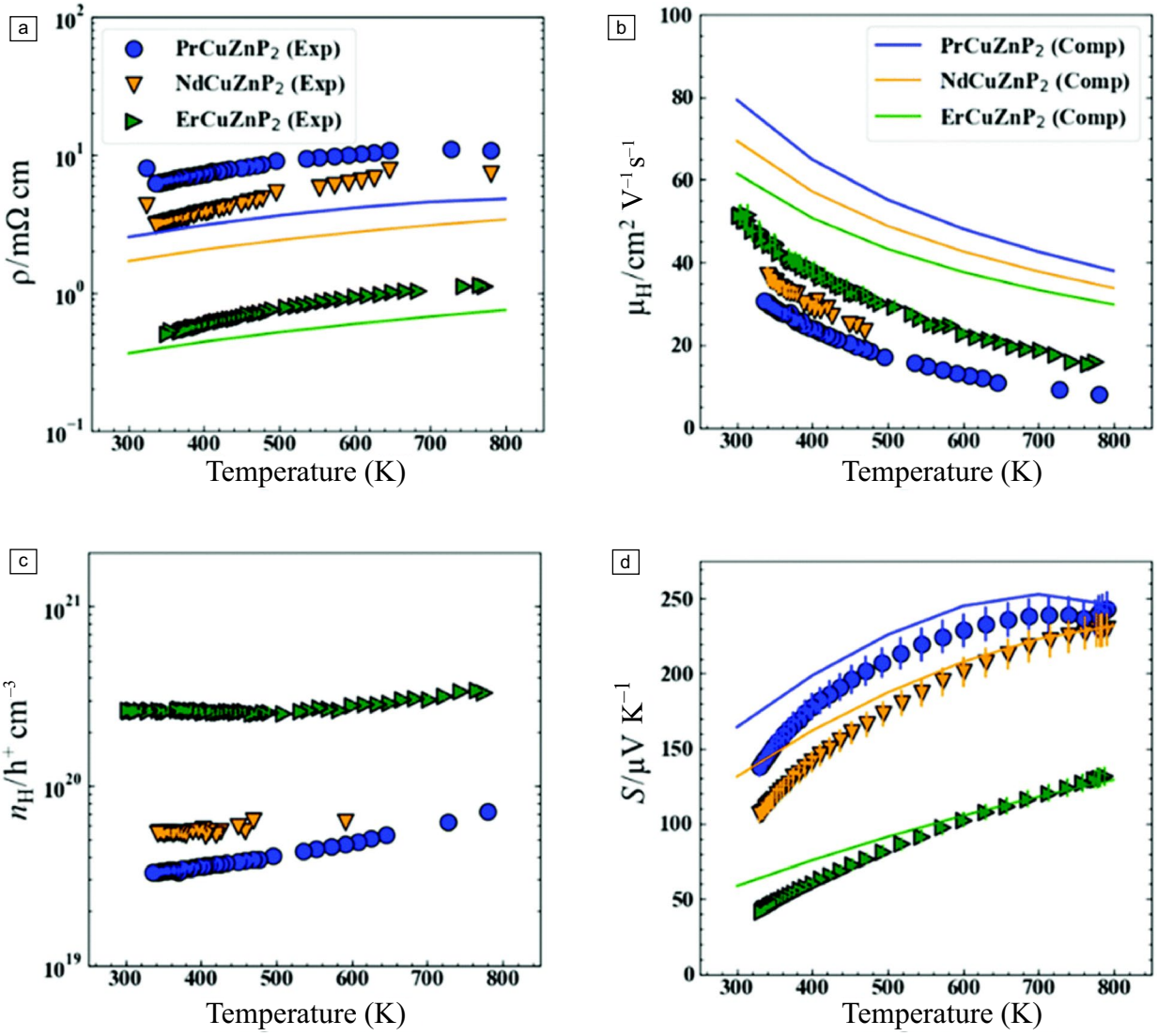

Figure 4. Recent advances in density functional theory-based calculations allow for the generation of computational training data for both the (a) resistivity and (b) mobility. From experimental carrier concentrations (c), the *Ab initio* Scattering and Transport (AMSET) method produces the (d) Seebeck coefficient.[7] This further highlights the need for defect calculations that predict carrier concentrations.

space using pretrained language models.[46] As shown in **Figure 5**a, using the Bidirectional Encoder Representations from Transformers model (BERT)-derived materials embeddings capture contextual knowledge of chemical and structural features, enabling similarity-based candidate retrieval and property prediction within a unified framework. This language-based recommendation system follows a two-step funnel architecture—candidate recall followed by property-based ranking—and incorporates a multitask mixture-of-experts model to improve predictive performance across multiple thermoelectric properties. As seen in Figure 5b–d, visualization tools based on dimensionality reduction such as the Uniform Manifold Approximation and Projection (UMAP) may reveal latent structure–property relationships, including "bands" of high-performing materials, that guide discovery in underexplored chemical spaces validated by first-principles calculations and experiments. Panel d illustrates how these embeddings naturally cluster chemically and structurally similar compounds, revealing trends that are less evident in traditional feature spaces.

Property prediction

A fundamental tension in materials discovery involves choosing between physics-constrained models for reliable extrapolation and flexible models optimized for accurate interpolation. With physics-constrained models, training data are fit using closed-form equations that retain some flexibility. Electronic mobility, for example, is strongly influenced by band mass but the combined effects of group velocity and scattering mechanisms make it difficult to assign a definitive exponent.[19]

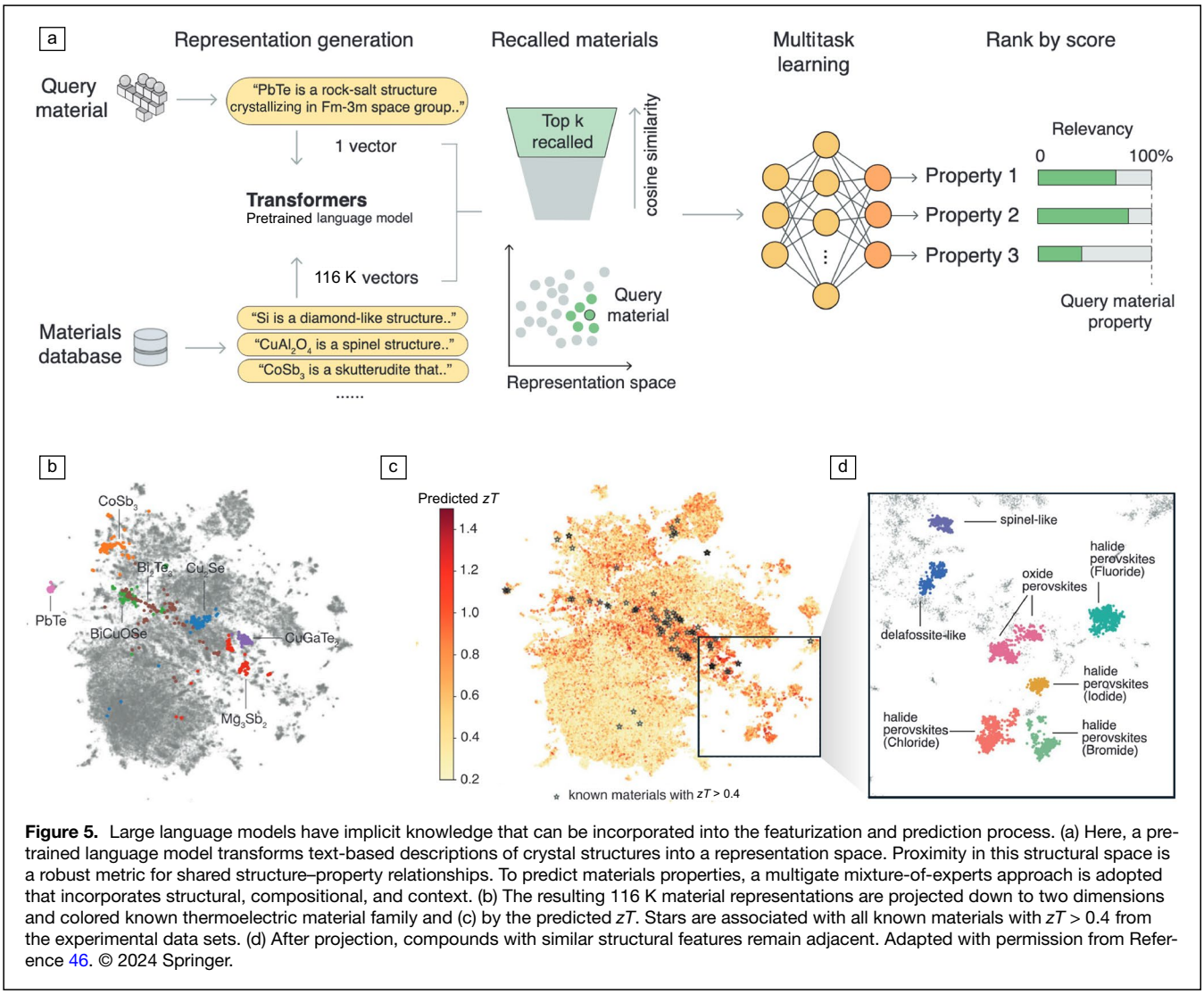

Figure 5. Large language models have implicit knowledge that can be incorporated into the featurization and prediction process. (a) Here, a pretrained language model transforms text-based descriptions of crystal structures into a representation space. Proximity in this structural space is a robust metric for shared structure–property relationships. To predict materials properties, a multigate mixture-of-experts approach is adopted that incorporates structural, compositional, and context. (b) The resulting 116 K material representations are projected down to two dimensions and colored known thermoelectric material family and (c) by the predicted zT. Stars are associated with all known materials with $zT > 0.4$ from the experimental data sets. (d) After projection, compounds with similar structural features remain adjacent. Adapted with permission from Reference 46. © 2024 Springer.

Physics-based models are also naturally suited to evolve in complexity by incorporating new physical descriptors.[21] For example, early models were ill-suited to predict charge transport in small gap semiconductors and semimetals, as they neglected the impact of minority carriers. Toriyama's model incorporated bandgap and the asymmetry of carrier transport into an analytic model, which led to the identification of novel candidate materials such as $SrSb_2$ and Zn_3As_2.[58] As a second example, secondary bands near the band edge are often present in structurally complex materials. These secondary bands can provide additional scattering channels and selectively lower the charge carrier relaxation time for high-energy charge carriers. Depending on their exact positioning, these secondary bands can deleteriously lower the electronic mobility or advantageously lower the Lorenz number. The development of descriptors that incorporate these effects allows for a further refinement of property predictions.[48]

More flexible, machine learning-based models, are appropriate when working with features that do not directly align with physics-based models (e.g., those derived from composition alone). Most common among these are ensemble learning algorithms, such as random forest, adaptive boosting, gradient boosting decision tree, and extreme gradient boosting.[2,43,52,53] In contrast, symbolic regression can be used to generate human-readable equations for a given property.[40] Finally, probabilistic or Bayesian regression approaches such as Gaussian process models provide a distribution over possible predictions, naturally capturing model uncertainty.[59]

From predictions to insight

Both the predictive models and extensive data sets produced through high-throughput screening can be mined for valuable insights into thermoelectric materials design. For instance, decision tree-based models that incorporate reciprocal space descriptors consistently identify key features such as effective mass, band degeneracy, and bandgap as top predictors of materials performance.[43] In contrast, models constructed without DFT-derived descriptors tend to be less consistent, often

highlighting seemingly unrelated or physically obscure features such as those derived from elemental melting points and electronegativities.[2] Models built using symbolic regression offer interpretability through explicit algebraic expressions involving features[40] but raise the question of whether generating such equations without a physical foundation provides meaningful insights. In contrast, physics-based models can offer similar flexibility while remaining directly interpretable and grounded in physical principles. Classical statistical techniques can also be applied to assess causal relationships within large data sets. For example, statistical significance tests have demonstrated a notable correlation between high TE quality factor β and the presence of specific chemical elements in large data sets of hypothetical half-Heusler compounds.[60]

For broader searches, however, extracting structural insights across different crystal structures still presents considerable challenges. Minor variations in atomic ordering or subtle distortions can cause structures to belong to different space groups, while conversely, materials with distinct overall structures may still share common sublattices or local motifs. Several approaches to material representation aim to address this complexity and enable meaningful insights across broader structural spaces. Local similarity methods such as smooth overlap of atomic positions (SOAP) quantitatively describe local atomic environments, while graph neural networks (GNNs) effectively capture both local and global structural relationships by treating materials as atomistic graphs.

From computation to experiment: Testing predictions

Despite the simplifications intrinsic to these models, some have proven to be extremely effective. For example, *n*-type Mg_3Sb_2 was predicted to be an excellent thermoelectric material before its ultimate realization.[19,61,62] Likewise, GeTe was identified as a promising binary semiconductor before the recent experimental successes seen in this material.[63,64] However, the absence of dopability considerations in screening has also led to many experimentalists working on compounds that ultimately proved fruitless. An early example is $TmAgTe_2$, where Tm_{Ag} antisite defects precluded the *p*-type doping necessary to achieve the predicted high performance.[65]

Beyond individual materials, high-throughput models have identified entire material classes that consistently exhibit chemistries predictive of high thermoelectric performance. This strategy acknowledges the inherent imprecision of calculations, while recognizing that broad trends can still provide valuable guidance to experimentalists. An early example of such meta-analysis is exemplified by the emergence of *n*-type Zintl compounds. Consistent with the earlier indication that *n*-type LiZnSb could be a high performance thermoelectric material,[11] high-throughput studies regularly revealed *n*-type Zintl compounds should possess high mobility. While *p*-type Zintl compounds such as $Yb_{14}MnSb_{11}$ and Ca_3AlSb_3 were well known, *n*-type analogs were largely unstudied. In retrospect, we now know that the prevalence of *p*-type Zintl compounds is due to the prevalence of cation vacancies that pin the Fermi level to the valence-band edge.[13,66,67] Experimental efforts to identify *n*-type select dopable Zintl compounds proved fruitful, with compounds such as $KAlSb_4$ emerging as early examples with excellent thermoelectric performance.[68–70]

Defects and dopants

After identifying a promising family of compounds, perhaps from high-throughput search, one could assume experimental realization is straightforward. However, this is rarely the case. More often than not, optimally positioning the Fermi level for thermoelectric performance proves to be a significant challenge, if not impossible. The last five years, however, have seen computational advances that render this design challenge more tractable and substantially reduce the burden for experimental realization.

To reiterate, thermoelectric materials require tuning the Fermi level to degenerate levels ($\geq 10^{19}$ cm^{-3}). This challenge is compounded by thermoelectric materials' structural complexity. With multiple cations and Wyckoff sites often present, the likelihood of forming one or more "killer defects" that compensate carriers or pin the Fermi level rises dramatically. Vacancies, interstitials, and antisites can each introduce deep donor or acceptor states, making it difficult–or even impossible–to dope some compounds above $\geq 10^{19}$ cm^{-3}. The structural complexity of thermoelectric materials often confounds the development of an intuition for dopability.

Experimentally derived training data for dopability are fraught; the available doping ranges found in the literature corpus reflect both thermodynamic limits and finite human effort.[72] Computational methods provide an alternative. In the mid-2010s, first-principles defect calculations of thermoelectric materials began to be widely adopted, driven by improvements in computational accuracy and growth in compute.[14,16] Further, the development of automated defect calculation workflows enabled the study of structural complex materials where dozens of distinct defect-charge state pairs needed to be considered.[15] To translate these calculations into experimental synthesis conditions, phase boundary mapping has proven invaluable.[73] Here, the multiphase invariant points serve to pin the elemental chemical potentials. Brouwer diagrams in chemical potential space likewise provide insight into the evolution of extrinsic dopant and native defect populations (**Figure 6**).[74]

To minimize spurious image interactions arising from periodic boundary conditions and simulate defects at the dilute limit, large supercells are typically employed. These large supercells help alleviate finite-size effects, but they come at a significant computational cost. As such, there has been interest in developing ML-based surrogates for defect energies. Early models used handcrafted features such as coordination number, electronegativity, and atomic size. By staying within narrow structural ranges (e.g., zinc-blende semiconductors), reasonably high accuracies could be achieved.[75] These interpretable models lacked the flexibility to capture long-range interactions, local disorder, or asymmetric coordination

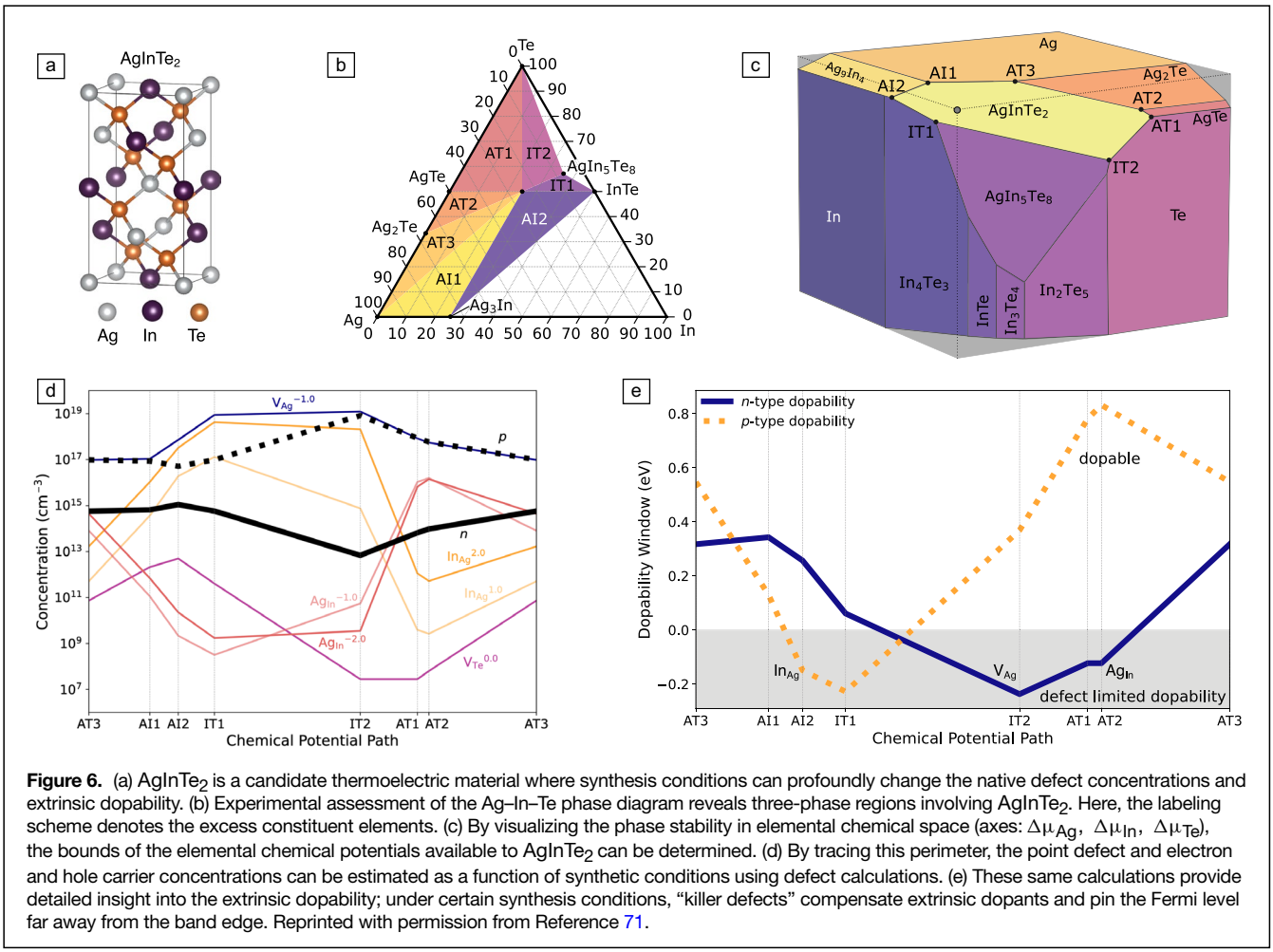

Figure 6. (a) $AgInTe_2$ is a candidate thermoelectric material where synthesis conditions can profoundly change the native defect concentrations and extrinsic dopability. (b) Experimental assessment of the Ag–In–Te phase diagram reveals three-phase regions involving $AgInTe_2$. Here, the labeling scheme denotes the excess constituent elements. (c) By visualizing the phase stability in elemental chemical space (axes: $\Delta\mu_{Ag}$, $\Delta\mu_{In}$, $\Delta\mu_{Te}$), the bounds of the elemental chemical potentials available to $AgInTe_2$ can be determined. (d) By tracing this perimeter, the point defect and electron and hole carrier concentrations can be estimated as a function of synthetic conditions using defect calculations. (e) These same calculations provide detailed insight into the extrinsic dopability; under certain synthesis conditions, "killer defects" compensate extrinsic dopants and pin the Fermi level far away from the band edge. Reprinted with permission from Reference 71.

environments, limiting their generalizability across diverse chemistries. Moreover, the sensitivity of predicted carrier concentrations to defect formation energies–especially in narrow-gap materials–places stringent accuracy requirements on the model, often on the order of 0.1 eV or less.

Graph neural networks are beginning to provide a useful alternative. They learn directly from bulk crystal structures and represent both atomic identity and bonding patterns.[76,77] These models avoid manual feature engineering and generalize across broader chemical spaces. They support site-specific predictions, enabling high-throughput evaluation across diverse structural motifs. Newer methods use machine-learned interatomic potentials (MLIPs) as surrogates to explore the potential energy surface, enabling the discovery of symmetry-broken, low-energy defect structures that traditional DFT methods often miss due to the high computational cost of sampling reconstructions.[78] These structures can strongly influence charge carrier dynamics, particularly in complex materials such as thermoelectrics, where metastable reconstructions can dominate formation energies and govern dopability windows. Limitations remain for these surrogate models; incorporating the energy from different charge states will be crucial for future work.[79] Furthermore, the accuracy of defect energies generated from surrogate models could remain a question in the absence of robust uncertainty quantification.

Alloys

Following the workflow in Figure 3a, once promising and dopable thermoelectric materials are discovered, they can be further optimized through alloying to tune the electronic structure and disrupt the transport of heat. Including one (or multiple) composition axis provides the continuous degree of freedom necessary for the precise chemical tuning necessary in thermoelectrics. Canonical examples include both aliovalent (e.g., Ag/Sb in GeTe) and isoelectronic (e.g., $PbTe_{1-x}Se_x$) alloys. As a side note, while alloying typically begins from high-performing parent materials, the $Si_{1-x}Ge_x$ system serves as an interesting counterexample.

Despite the promise of multi-property compositional tuning, discovering high-performing alloys poses its own set of challenges. Due to the disorder intrinsic in alloys, it is far more difficult to simulate alloy properties, structure, or even

thermodynamic stability. Furthermore, alloys could exhibit ordering tendencies arising from local sterics and electrostatics.[80,81] Synergistic effects between alloying elements further compounds the challenge as multicomponent alloys[82,83] both expand the composition search space and lead to a combinatorial explosion in local structural motifs. Below, we break up these challenges into the assessment of phase stability and the subsequent prediction of transport properties. Critically, AI/ML techniques are emerging to address issues of synthesis, structure, and transport, building the foundation necessary for high-throughput screenings of thermoelectric alloys.

Phase stability

A prerequisite to transport predictions is determining the stability and structure of an alloy. Without these predictions, further calculations on alloy transport properties risk (1) being erroneous because they use the wrong structure; or (2) irrelevant by falsely assuming an alloy is stable. Special quasi-random structures are used to approximate an alloy as a fully disordered material with a single, large supercell,[84–86] while the independent cell approximation represents the alloy as an ensemble of small, ordered configurational states to ease computational scaling costs.[87–90] Both approaches allow for the approximation of local structure and configurational free energies from first principles.

If significant degrees of short-range order are expected, such as in aliovalent alloys,[81] then surrogate models such as cluster expansion or an MLIP are useful for exploring the vast configurational space.[91–93] A cluster expansion is a model Hamiltonian fit based on DFT calculations to predict alloy energies based on the configuration of atoms on a disordered lattice. With a relatively cheap energy surrogate, Monte Carlo-based sampling reveals the local structure (i.e., motifs) and the configurational free energy for a given temeperature.[94,95] The resulting free energies can then be leveraged to produce a free energy convex hull in order to assess phase stability. Regardless of the energy surrogate model, active learning methods are useful for minimizing the number of thermodynamic calculations necessary to determine alloy phase stability.[96–98] Finally, it is worth noting that this discussion has revolved only on static structure; we envision a future where the widespread use of MLIPs allows for the incorporation of dynamics into alloy simulation, impacting our understanding of local structure, motif populations, and vibrational contributions to thermodynamic stability.[99]

Transport in alloys

With stability and local ordering tendencies established, we can evaluate transport properties. Ideally, the impact of alloying is strictly perturbative on the electronic structure to maintain high carrier mobility. For example, **Figure 7**a considers the impact of alloying GeTe and SnTe on the electronic structure. Here, supercell calculations are unfolded into the primitive Brillouin zone, leading to a noninteger spectral weight. In this case, the bands exhibit minimal smearing and the mobility is only modestly affected. In contrast, the addition of Mn (Figure 7b) causes a massive breakdown in the band sharpness, associated with k no longer being a good quantum number.[86] Consistent with these predictions, Mn is known to significantly increase the experimental effective mass of GeTe upon alloying ($1m_e$ to $12m_e$).

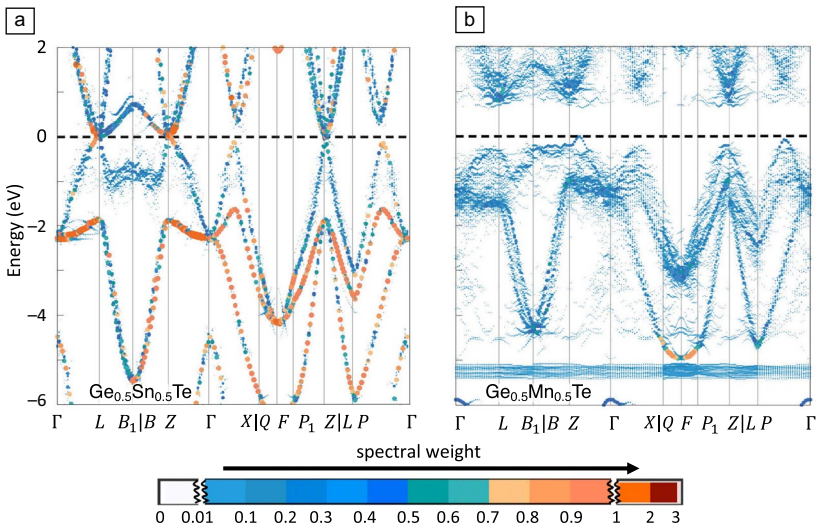

Figure 7. Alloys can be approximated as supercells; unfolding the resulting electronic structure back to the primitive Brillouin zone induces spectral smearing. (a) Here, we see that alloying GeTe with Sn has minimal impact on the electronic structure and the spectral weight remains sharp. (b) In contrast, alloying Ge with Mn induces significant smearing, indicating a breakdown of k as a good quantum number.[86]

At the same time, we seek alloys that are so disruptive to heat transport that a phononic view may no longer apply. For the latter, machine-learned interatomic potentials (MLIPs) enable access to regimes where standard lattice dynamics breaks down, offering tractable paths to simulate vibrational behavior in disordered, anharmonic, or glass-like materials. Several approaches are in principle now available: (1) Green–Kubo methods using MLIP-driven molecular dynamics provide the most direct access to incoherent heat transport and require no assumptions about phonon quasiparticles; (2) the stochastic self-consistent harmonic approximation[100] (SSCHA) incorporates nonperturbative anharmonic renormalization and can feed into Boltzmann transport or Green–Kubo formalisms; and (3) temperature-dependent effective potential (TDEP) methods, while less rigorous, yield effective interatomic

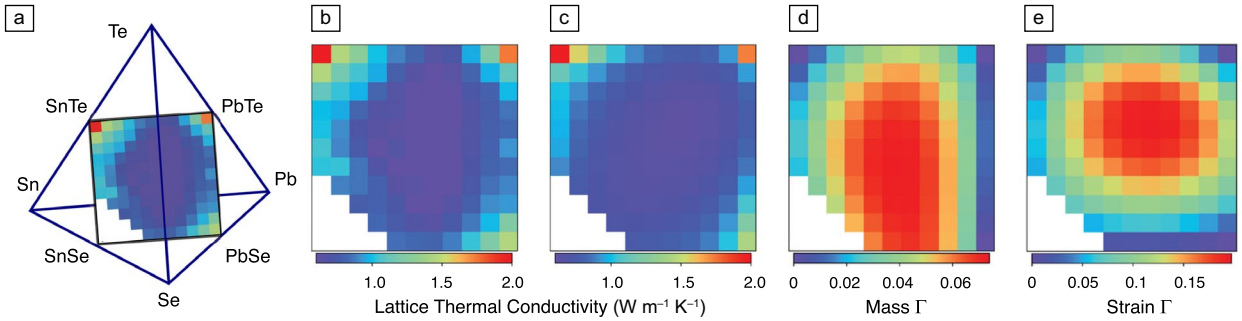

Figure 8. (a) The (Sn, Pb)(Se, Te) rock-salt subspace lives within the larger Sn–Pb–Se–Te quaternary phase diagram. (b) Experimental results are well-fit with (c) physics-based models. By retaining interpretability, the relative contributions of (d) mass and (e) strain scattering emerge. Here, the strain scattering dominates for all alloy compositions. Reprinted with permission from Reference 103.

force constants and phonon lifetimes at finite temperature with broad applicability across alloys.[101] For example, in disordered wurtzite ScAlN alloys, a neuro-evolution MLIP was trained to first-principles accuracy and used to compute lattice thermal conductivity.[102] Combined use of the Allen–Feldman framework and homogeneous nonequilibrium molecular dynamics simulations revealed the temperature-driven transition from phonon-like propagons to incoherent, diffusive vibrational modes.

While alloy calculations for both heat and charge transport continue to see a major revolution, ultimately the cost of exhaustively enumerating these calculations for every composition will remain overwhelming, if not wasteful. High-level analytical models are available to interpolate transport properties as a function of composition. Consistent with the previous discussion, regression can either be accomplished through more rigid, physics-based models or more flexible machine learning models. For example, **Figure** 8 highlights an analytic model that closely captures the underlying physics of lattice thermal conductivity in a multicomponent alloy.[103] The interpretable nature of these models allows for the decomposition of constituent scattering mechanisms. Future work could incorporate active learning algorithms to minimize the number of transport calculations necessary to fit these analytical models.

Conclusion

In this dizzying high-dimensional design space we call thermoelectrics, there are a variety of ways in which a promising candidate material could turn out to be unfruitful. Indeed, we have fallen into many of these pitfalls while using high-throughput search. As we have outlined, candidates have turned out not to be synthesizable, or even if they could be made, "killer defects" prevented them from being sufficiently dopable. In the fortunate scenario when a material could be synthesized and its defects controlled, errors in the computationally predicted transport properties often compounded, ultimately producing mediocre results when explored experimentally.

There is no simple solution for perfecting high-throughput screening, but we have outlined several key areas where ongoing improvements continue to advance the field. Better computational methods allow for a more in-depth treatment of electron and phonon scattering, while high-throughput defect calculations remain indispensable for assessing dopability. Also, first-principles alloy calculations and active learning methods are beginning to provide methods for assessing stability and structure across continuous composition spaces. Coupling libraries of stable alloys with high-throughput screening methods and analytic transport models will be an exciting area of future research.

No discussion of machine learning in materials science would be complete without mentioning machine-learned interatomic potentials. These surrogate models hold promise for accelerating progress across multiple domains of materials discovery, including the evaluation of stability, synthesizability, dopability, and thermal transport. However, as a community, we must rigorously benchmark and validate these models to build trust in their applicability and to understand their limitations–similar to the collective effort that established the credibility of DFT in the 1990s and 2000s, and hybrid functionals in the early 2010s.

Stepping back, high-throughput methods are useful tools that sacrifice (hopefully small) degrees of accuracy for large gains in computational efficiency, allowing for the screening of vast numbers of candidates. Within thermoelectrics, these searches often resemble the top portion of the hourglass in Figure 3a. However, in the bottom half of the hourglass–where select candidates are optimized–the dichotomy between computational quantity and quality begins to collapse. The quality of our computational assessments is often limited by the quantity of conditions, atoms, or time steps we can conduct. For instance, evaluating dopability is the act of calculating many defect energies. Understanding the stability of alloys requires evaluating many free energies across composition space. And predicting thermal properties necessitates running simulations for longer time scales. While high-throughput and ML approaches have provided aid for preliminary thermoelectric screening, we are truly excited to see them starting to enable an atomistic understanding of materials chemistry and physics. Through the use of simulation at larger length scales, longer time scales, and

under more realistic conditions, we envision a future where the combination of computation and experiment can serve to bring increasingly deep insight into the foundational materials science on which thermoelectric discovery is predicated.

Author contributions

E.S.T. conceived the concept of this article with input from all authors. All authors prepared the figures and wrote the manuscript.

Funding

The authors acknowledge the support of NSF OAC 2118201.

Conflict of interest

On behalf of all authors, the corresponding author states that there is no conflict of interest.

References

1. S. Hachmioune, A.M. Ganose, M.B. Sullivan, D.O. Scanlon, *Chem. Mater.* **36**(12), 6062 (2024)
2. M. Al-Fahdi, K. Yuan, Y. Yao, R. Rurali, M. Hu, *Appl. Phys. Rev.* **11**(2), 021402 (2024)
3. H. Wang, J. Wang, X. Cao, G.J. Snyder, *J. Mater. Chem. A* **2**(9), 3169 (2014)
4. S. Wang, G. Zheng, T. Luo, X. She, H. Li, X. Tang, *J. Phys. Appl. Phys.* **44**(47), 475304 (2011)
5. K. Imasato, C. Fu, Y. Pan, M. Wood, J.J. Kuo, C. Felser, G.J. Snyder, *Adv. Mater.* **32**(16), 1908218 (2020)
6. L. Song, J. Zhang, B.B. Iversen, *J. Mater. Chem. A* **5**(10), 4932 (2017)
7. J.-H. Pöhls, S. Chanakian, J. Park, A.M. Ganose, A. Dunn, N. Friesen, A. Bhattacharya, B. Hogan, S. Bux, A. Jain, *Mater. Horiz.* **8**(1), 209 (2021)
8. Y. Zheng, S. Wang, W. Liu, Z. Yin, H. Li, X. Tang, C. Uher, *J. Phys. D Appl. Phys.* **47**(11), 115303 (2014)
9. W. Li, J. Carrete, N.A. Katcho, N. Mingo, *Comput. Phys. Commun.* **185**(6), 1747 (2014). https://doi.org/10.1016/j.cpc.2014.02.015
10. G.K.H. Madsen, D.J. Singh, Boltztrap. *Comput. Phys. Commun.* **175**(1), 67 (2006). https://doi.org/10.1016/j.cpc.2006.03.007
11. G.K.H. Madsen, *J. Am. Chem. Soc.* **128**(37), 12140 (2006). https://doi.org/10.1021/ja062526a
12. E.S. Toberer, A.F. May, C.J. Scanlon, G.J. Snyder, *J. Appl. Phys.* **105**(6), 063701 (2009). https://doi.org/10.1063/1.3091267
13. P. Gorai, A. Goyal, E.S. Toberer, V. Stevanović, *J. Mater. Chem. A* **7**, 19385 (2019). https://doi.org/10.1039/C9TA03786A
14. V. Stevanović, S. Lany, X. Zhang, A. Zunger, *Phys. Rev. B* **85**, 115104 (2012). https://doi.org/10.1103/PhysRevB.85.115104
15. A. Goyal, P. Gorai, H. Peng, S. Lany, V. Stevanović, *Comput. Mater. Sci.* **130**, 1 (2017)
16. A. Jain, G. Hautier, S.P. Ong, C.J. Moore, C.C. Fischer, K.A. Persson, G. Ceder, *Phys. Rev. B* **84**, 045115 (2011). https://doi.org/10.1103/PhysRevB.84.045115
17. S. Curtarolo, G.L.W. Hart, M.B. Nardelli, N. Mingo, S. Sanvito, O. Levy, *Nat. Mater.* **12**(3), 191 (2013). https://doi.org/10.1038/nmat3568
18. S. Wang, Z. Wang, W. Setyawan, N. Mingo, S. Curtarolo, *Phys. Rev. X* **1**, 021012 (2011). https://doi.org/10.1103/PhysRevX.1.021012
19. J. Yan, P. Gorai, B. Ortiz, S. Miller, S.A. Barnett, T. Mason, V. Stevanović, E.S. Toberer, *Energy Environ. Sci.* **8**, 983 (2015). https://doi.org/10.1039/C4EE03157A
20. L. Xi, S. Pan, X. Li, Y. Xu, J. Ni, X. Sun, J. Yang, J. Luo, J. Xi, W. Zhu, X. Li, D. Jiang, R. Dronskowski, X. Shi, G.J. Snyder, W. Zhang, *J. Am. Chem. Soc.* **140**(34), 10785 (2018). https://doi.org/10.1021/jacs.8b04704
21. P. Gorai, V. Stevanović, E.S. Toberer, *Nat. Rev. Mater.* **2**(9), 17053 (2017). https://doi.org/10.1038/natrevmats.2017.53
22. A. Merchant, S. Batzner, S.S. Schoenholz, M. Aykol, G. Cheon, E.D. Cubuk, *Nature* **624**(7990), 80 (2023). https://doi.org/10.1038/s41586-023-06735-9
23. A.M. Ochs, P. Gorai, Y. Wang, M.R. Scudder, K. Koster, C.E. Moore, V. Stevanović, J.P. Heremans, W. Windl, E.S. Toberer, J.E. Goldberger, *Chem. Mater.* **33**(3), 946 (2021). https://doi.org/10.1021/acs.chemmater.0c04030
24. F. Garmroudi, M. Parzer, A. Riss, C. Bourgès, S. Khmelevskyi, T. Mori, E. Bauer, A. Pustogow, *Sci. Adv.* **9**(37), 1611 (2023). https://doi.org/10.1126/sciadv.adj1611
25. P. Gorai, A. Ganose, A. Faghaninia, A. Jain, V. Stevanović, *Mater. Horiz.* **7**(7), 1809 (2020). https://doi.org/10.1039/D0MH00197J
26. J. Qu, V. Stevanović E. Ertekin, P. Gorai, *J. Mater. Chem. A* **8**(47), 25306 (2020). https://doi.org/10.1039/D0TA08238D
27. F. Therrien, E.B. Jones, V. Stevanović, *Appl. Phys. Rev.* **8**(3), 031310 (2021). https://doi.org/10.1063/5.0049453
28. V. Stevanović, *Phys. Rev. Lett.* **116**, 075503 (2016). https://doi.org/10.1103/PhysRevLett.116.075503
29. C.J. Pickard, R.J. Needs *J. Phys. Condens. Matter* **23**(5), 053201 (2011). https://doi.org/10.1088/0953-8984/23/5/053201
30. A. Novick, Q. Nguyen, M. Jankousky, M.B. Tellekamp, E.S. Toberer, V. Stevanović *J. Am. Chem. Soc.* **147**, 4419 (2025)
31. T. Xie, X. Fu, O.-E. Ganea, R. Barzilay, T.S. Jaakkola, "Crystal Diffusion Variational Autoencoder for Periodic Material Generation," *Tenth International Conference on Learning Representations (ICLR 2022)* (Virtual) (April 25–29, 2022), Paper 1120
32. R. Jiao, W. Huang, P. Lin, J. Han, P. Chen, Y. Lu, Y. Liu, "Crystal Structure Prediction by Joint Equivariant Diffusion," *Thirty-Seventh Annual Conference on Neural Information Processing Systems (NeurIPS 2023)*, (New Orleans, December 10–16, 2023), no. 2730. https://openreview.net/forum?id=DNdN26m2Jk
33. C. Zeni, R. Pinsler, D. Zügner, A. Fowler, M. Horton, X. Fu, Z. Wang, A. Shysheya, J. Crabbé, S. Ueda, R. Sordillo, L. Sun, J. Smith, B. Nguyen, H. Schulz, S. Lewis, C.-W. Huang, Z. Lu, Y. Zhou, H. Yang, H. Hao, J. Li, C. Yang, W. Li, R. Tomioka, T. Xie, *Nature* **639**, 624 (2025). https://doi.org/10.1038/s41586-025-08628-5
34. Y. Lipman, R.T.Q. Chen, H. Ben-Hamu, M. Nickel, M. Le, "Flow Matching for Generative Modeling," *Eleventh International Conference on Learning Representations (ICLR 2023)* (Kigali, May 1–5, 2023), Paper 3719. https://openreview.net/forum?id=PqvMRDCJT9t
35. A. Jain, S.P. Ong, G. Hautier, W. Chen, W.D. Richards, S. Dacek, S. Cholia, D. Gunter, D. Skinner, G. Ceder, *APL Mater.* **1**(1), 011002 (2013). https://doi.org/10.1063/1.4812323
36. J.E. Saal, S. Kirklin, M. Aykol, B. Meredig, C. Wolverton, *JOM* **65**, 1501 (2013)
37. S. Curtarolo, W. Setyawan, S. Wang, J. Xue, K. Yang, R.H. Taylor, L.J. Nelson, G.L. Hart, S. Sanvito, M. Buongiorno-Nardelli, N. Mingo, O. Levy, *Comput. Mater. Sci.* **58**, 2275 (2012)
38. K. Choudhary, K.F. Garrity, A.C. Reid, B. DeCost, A.J. Biacchi, A.R.H. Walker, Z. Trautt, J. Hattrick-Simpers, A.G. Kusne, A. Centrone, A. Davydov, *NPJ Comput. Mater.* **6**(1), 173 (2020)
39. C. Draxl, M. Scheffler, *J. Phys. Mater.* **2**(3), 036001 (2019)
40. T.A. Purcell, M. Scheffler, L.M. Ghiringhelli, C. Carbogno, *NPJ Comput. Mater.* **9**(1), 112 (2023)
41. Y. Katsura, M.K.T. Kodani, M. Kaneshige, Y. Ando, S. Gunji, Y. Imai, K.T.H. Ouchi, K. Kimura, K. Tsuda, *Sci. Technol. Adv. Mater.* **20**(1), 511 (2019). https://doi.org/10.1080/14686996.2019.1603885
42. T. Zhu, R. He, S. Gong, T. Xie, P. Gorai, K. Nielsch, J.C. Grossman, *Energy Environ. Sci.* **14**(7), 3559 (2021). https://doi.org/10.1039/D1EE00442E
43. T. Fan, A.R. Oganov, *J. Mater. Chem. C* **13**(3), 1439 (2025). https://doi.org/10.1039/D4TC03403A
44. J. Park, A.M. Ganose, Y. Xia, *Appl. Phys. Rev.* **12**(1), 011339 (2025). https://doi.org/10.1063/5.0241645
45. A.M. Ganose, J. Park, A. Faghaninia, R. Woods-Robinson, K.A. Persson, A. Jain, *Nat. Commun.* **12**(1), 2222 (2021). https://doi.org/10.1038/s41467-021-22440-5
46. J. Qu, Y.R. Xie, K.M. Ciesielski, C.E. Porter, E.S. Toberer, E. Ertekin, *NPJ Comput. Mater.* **10**(1), 58 (2024). https://doi.org/10.1038/s41524-024-01231-8
47. Z.M. Gibbs, F. Ricci, G. Li, H. Zhu, K. Persson, G. Ceder, G. Hautier, A. Jain, G.J. Snyder, *NPJ Comput. Mater.* **3**(1), 8 (2017). https://doi.org/10.1038/s41524-017-0013-3
48. R.W. McKinney, P. Gorai, V. Stevanović, E.S. Toberer, *J. Mater. Chem. A* **5**, 17302 (2017). https://doi.org/10.1039/C7TA04332E
49. Y. Wu, L. Ji, Y. Ding, L. Zhou, *Mater. Horiz.* **11**, 3651 (2024). https://doi.org/10.1039/D4MH00363B
50. J. Yuan, Y. Chen, B. Liao, *J. Am. Chem. Soc.* **145**(33), 18506 (2023). https://doi.org/10.1021/jacs.3c05091
51. E.B. Isaacs, G.M. Lu, C. Wolverton, *J. Phys. Chem. Lett.* **11**(14), 5577 (2020). https://doi.org/10.1021/acs.jpclett.0c01077
52. Q. Ren, B. Zhu, G. Tang, J. Hong, *Small* **21**, 2412745 (2025)
53. Y. Liu, Z. Mu, P. Hong, Y. Yang, C. Lin, *Nanoscale* **17**(4), 2200 (2025)
54. T. Xie, J.C. Grossman, *Phys. Rev. Lett.* **120**(14), 145301 (2018)
55. M. Geiger, T. Smidt, e3nn: Euclidean neural networks (2022), Preprint, https://arxiv.org/abs/2207.09453
56. S. Batzner, A. Musaelian, L. Sun, M. Geiger, J.P. Mailoa, M. Kornbluth, N. Molinari, T.E. Smidt, B. Kozinsky, *Nat. Commun.* **13**(1), 2453 (2022). https://doi.org/10.1038/s41467-022-29939-5
57. S. Batzner, A. Musaelian, B. Kozinsky, *Nat. Rev. Phys.* **5**(8), 437 (2023). https://doi.org/10.1038/s42254-023-00615-x
58. M.Y. Toriyama, A.N. Carranco, G.J. Snyder, P. Gorai, *Mater. Horiz.* **10**(10), 4256 (2023). https://doi.org/10.1039/D3MH01013A
59. V.L. Deringer, A.P. Bartók, N. Bernstein, D.M. Wilkins, M. Ceriotti, G. Csányi, *Chem. Rev.* **121**(16), 10073 (2021)
60. A. Pak, K. Ciesielski, M. Wróblewska, E.S. Toberer, E. Ertekin, Mapping the configuration space of half-Heusler compounds via subspace identification for thermoelectric materials discovery (2025), Preprint, https://arxiv.org/abs/2501.11644
61. H. Tamaki, H.K. Sato, T. Kanno, *Adv. Mater.* **28**(46), 10182 (2016)
62. S. Ohno, K. Imasato, S. Anand, H. Tamaki, S.D. Kang, P. Gorai, H.K. Sato, E.S. Toberer, T. Kanno, G.J. Snyder, *Joule* **2**(1), 141 (2018)
63. P. Gorai, P. Parilla, E.S. Toberer, V. Stevanović, *Chem. Mater.* **27**(18), 6213 (2015). https://doi.org/10.1021/acs.chemmater.5b01179

64. X. Zhang, Z. Bu, S. Lin, Z. Chen, W. Li, Y. Pei, *Joule* **4**(5), 986 (2020). https://doi.org/10.1016/j.joule.2020.03.004
65. H. Zhu, G. Hautier, U. Aydemir, Z.M. Gibbs, G. Li, S. Bajaj, J.-H. Pöhls, D. Broberg, W. Chen, A. Jain, M.A. White, M. Asta, G.J. Snyder, K. Persson, G. Ceder, *J. Mater. Chem. C* **3**, 10554 (2015). https://doi.org/10.1039/C5TC01440A
66. S.M. Kauzlarich, A. Zevalkink, E. Toberer, G.J. Snyder, "Zintl Phases: Recent Developments in Thermoelectrics and Future Outlook," in *Thermoelectric Materials and Devices*, ed. by I. Nandhakumar, N.M. White, S. Beeby, Energy and Environment Series (Royal Society of Chemistry, 2016), chap. 1, pp. 1–26. https://doi.org/10.1039/9781782624042-00001
67. E.S. Toberer, A.F. May, G.J. Snyder, *Chem. Mater.* **22**(3), 624 (2010). https://doi.org/10.1021/cm901956r
68. B.R. Ortiz, P. Gorai, L. Krishna, R. Mow, A. Lopez, R. McKinney, V. Stevanović, E.S. Toberer, *J. Mater. Chem. A* **5**, 4036 (2017). https://doi.org/10.1039/C6TA09532A
69. S. Baranets, T. Kandabadage, X. Wang, X. Bai, D.P. Young, S. Bobev, *Chem. Mater.* **36**(15), 7570 (2024). https://doi.org/10.1021/acs.chemmater.4c01669
70. Z. Zhang, J. Li, H. Yao, Q. Wang, L. Yin, K. Liu, X. Ma, M. Yuan, R. Wang, S. Duan, X. Bao, J. Cheng, X. Wang, X. Li, J. Shuai, J. Sui, X. Lin, X. Tan, X. Liu, J. Mao, G. Xie, Q. Zhang, *Acta Mater.* **268**, 119777 (2024). https://doi.org/10.1016/j.actamat.2024.119777
71. V. Meschke, L.C. Gomes, J.M. Adamczyk, K.M. Ciesielski, C.M. Crawford, H. Vinton, E. Ertekin, E.S. Toberer, *J. Mater. Chem. C* **11**, 3832 (2023). https://doi.org/10.1039/D3TC00070B
72. S.A. Miller, M. Dylla, S. Anand, K. Gordiz, G.J. Snyder, E.S. Toberer, *NPJ Comput. Mater.* **4**(1), 71 (2018). https://doi.org/10.1038/s41524-018-0123-6
73. L. Borgsmiller, D. Zavanelli, G.J. Snyder, *PRX Energy* **1**(2), 022001 (2022). https://doi.org/10.1103/PRXEnergy.1.022001
74. S. Anand, M.Y. Toriyama, C. Wolverton, S.M. Haile, G.J. Snyder, *Acc. Mater. Res.* **3**(7), 685 (2022). https://doi.org/10.1021/accountsmr.2c00044
75. A. Mannodi-Kanakkithodi, X. Xiang, L. Jacoby, R. Biegaj, S.T. Dunham, D.R. Gamelin, M.K.Y. Chan, *Patterns* **3**(3), 100450 (2022). https://doi.org/10.1016/j.patter.2022.100450
76. M.H. Rahman, P. Gollapalli, P. Manganaris, S.K. Yadav, G. Pilania, B. DeCost, K. Choudhary, A. Mannodi-Kanakkithodi, *APL Mach. Learn.* **2**(1), 016122 (2024). https://doi.org/10.1063/5.0176333
77. M.D. Witman, A. Goyal, T. Ogitsu, A.H. McDaniel, S. Lany, *Nat. Comput. Sci.* **3**(8), 675 (2023). https://doi.org/10.1038/s43588-023-00495-2
78. I. Mosquera-Lois, S.R. Kavanagh, A.M. Ganose, A. Walsh, *NPJ Comput. Mater.* **10**(1), 121 (2024). https://doi.org/10.1038/s41524-024-01303-9
79. B. Deng, P. Zhong, K. Jun, J. Riebesell, K. Han, C.J. Bartel, G. Ceder, *Nat. Mach. Intell.* **5**(9), 1031 (2023). https://doi.org/10.1038/s42256-023-00716-3
80. A. Simonov, A.L. Goodwin, *Nat. Rev. Chem.* **4**(12), 657 (2020)
81. R.R. Schnepf, J.J. Cordell, M.B. Tellekamp, C.L. Melamed, A.L. Greenaway, A. Mis, G.L. Brennecka, S. Christensen, G.J. Tucker, E.S. Toberer, S. Lany, AC. Tamboli, *ACS Energy Lett.* **5**(6), 2027 (2020)
82. B. Jiang, Y. Yu, J. Cui, X. Liu, L. Xie, J. Liao, Q. Zhang, Y. Huang, S. Ning, B. Jia, B. Zhu, S. Bai, L. Chen, SJ. Pennycook, J. He, *Science* **371**(6531), 830 (2021)
83. Y. Liu, H. Xie, Z. Li, R. Dos Reis, J. Li, X. Hu, P. Meza, M. AlMalki, G.J. Snyder, M.A. Grayson, C. Wolverton, M.G. Kanatzidis, V.P. Dravid, *J. Am. Chem. Soc.* **146**(18), 12620 (2024)
84. A. Zunger, S. Wei, L.G. Ferreira, J.E. Bernard, *Phys. Rev. Lett.* **65**(3), 353 (1990)
85. J.W. Doak, C. Wolverton, *Phys. Rev. B Condens. Matter Mater. Phys.* **86**(14), 144202 (2012)
86. J.M. Adamczyk, F.A. Bipasha, G.A. Rome, K. Ciesielski, E. Ertekin, E.S. Toberer, *J. Mater. Chem. A* **10**, 16468 (2022)
87. C. Jiang, B.P. Uberuaga, *Phys. Rev. Lett.* **116**(10), 105501 (2016)
88. V. Sorkin, Z. Yu, S. Chen, T.L. Tan, Z. Aitken, Y. Zhang, *Sci. Rep.* **12**(1), 11894 (2022)
89. A. Novick, Q. Nguyen, R. Garnett, E. Toberer, V. Stevanović, *Phys. Rev. Mater.* **7**(6), 063801 (2023)
90. V. Meschke, A. Novick, J. Rogers, C. Porter, R. Chang, T. Proffen, E.S. Toberer, *J. Mater. Chem. C* **12**(35), 13863 (2024)
91. S. Kadkhodaei, J.A. Muñoz, *JOM* **73**(11), 3326 (2021)
92. K. Gubaev, E.V. Podryabinkin, G.L. Hart, A.V. Shapeev, *Comput. Mater. Sci.* **156**, 148 (2019)
93. J. Laakso, M. Todorović, J. Li, G.-X. Zhang, P. Rinke, *Phys. Rev. Mater.* **6**(11), 113801 (2022)
94. J.J. Cordell, J. Pan, A.C. Tamboli, G.J. Tucker, S. Lany, *Phys. Rev. Mater.* **5**(2), 024604 (2021)
95. J.J. Cordell, G.J. Tucker, A. Tamboli, S. Lany, *APL Mater.* **10**, 011112 (2022)
96. A. Vasylenko, B.M. Asher, C.M. Collins, M.W. Gaultois, G.R. Darling, M.S. Dyer, M.J. Rosseinsky, *J. Chem. Phys.* **160**(5), 054110 (2024)
97. D. Wen, V. Tucker, M.S. Titus, *NPJ Comput. Mater.* **10**(1), 210 (2024)
98. A. Novick, D. Cai, Q. Nguyen, R. Garnett, R. Adams, E. Toberer, *Mater. Horiz.* **11**, 5381 (2024). https://doi.org/10.1039/D4MH00432A
99. A. van De Walle, G. Ceder, *Rev. Mod. Phys.* **74**(1), 11 (2002)
100. I. Errea, M. Calandra, F. Mauri, *Phys. Rev. B* **89**, 064302 (2014). https://doi.org/10.1103/PhysRevB.89.064302
101. S.S. Das, S.N. Sadeghi, K. Esfarjani, M. Zebarjadi, *J. Mater. Chem. A* **12**, 14072 (2024). https://doi.org/10.1039/D4TA01088D
102. H. Dong, Z. Li, B. Sun, Y. Zhou, L. Liu, J.-Y. Yang, *Mater. Today Commun.* **39**, 109213 (2024). https://doi.org/10.1016/j.mtcomm.2024.109213
103. R. Gurunathan, S. Sarker, C.K.H. Borg, J. Saal, L. Ward, A. Mehta, G.J. Snyder, *Adv. Electron. Mater.* **8**(10), 2200327 (2022). https://doi.org/10.1002/aelm.202200327

Publisher's note
Springer Nature remains neutral with regard to jurisdictional claims in published maps and institutional affiliations.

Springer Nature or its licensor (e.g. a society or other partner) holds exclusive rights to this article under a publishing agreement with the author(s) or other rightsholder(s); author self-archiving of the accepted manuscript version of this article is solely governed by the terms of such publishing agreement and applicable law.

Eric S. Toberer is a professor of physics at the Colorado School of Mines. His work is at the intersection of computational and experimental materials science, with a focus on semiconductors for energy applications. For these efforts, he received the Presidential Early Career Award for Scientists and Engineers. He received his PhD degree in materials from the University of California, Santa Barbara, and was introduced to thermoelectric research while a postdoctoral scholar at the California Institute of Technology. Toberer can be reached by email at etoberer@mines.edu.

Andrew Novick is a postdoctoral fellow at Princeton University in the Department of Computer Science. His work focuses on developing new machine learning approaches that harness physical insights to address challenges in materials science. He received his PhD degree from the Colorado School of Mines in materials science and studied chemistry as an undergraduate at Washington University in St. Louis. Novick can be reached by email at novick@mines.edu.

Elif Ertekin is an associate professor, Andersen Faculty Scholar, and director of Mechanics Programs in the Department of Mechanical Science and Engineering at the University of Illinois at Urbana-Champaign (UIUC). She focuses on using computation, modeling, and simulation to develop a microscopic understanding of atomic and electronic scale processes in materials, with applications areas in thermal transport, energy conversion, and defect chemistry in solid-state materials. She received her PhD degree in materials science and engineering from the University of California, Berkeley, and carried out postdoctoral work at the Berkeley Nanoscience and Nanoengineering Institute and the Massachusetts Institute of Technology before moving to Illinois. Ertekin can be reached by email at ertekin@illinois.edu.